Eur Radiol (2018) 28:1551–1559
https://doi.org/10.1007/s00330-017-5119-y

HEPATOBILIARY-PANCREAS

Extracellular contrast agent-enhanced MRI: 15-min delayed phase may improve the diagnostic performance for hepatocellular carcinoma in patients with chronic liver disease

Si Eun Lee[1] · Chansik An[1] · Shin Hye Hwang[1] · Jin-Young Choi[1] · Kyunghwa Han[1] · Myeong-Jin Kim[1]

Received: 26 June 2017 / Revised: 27 September 2017 / Accepted: 3 October 2017 / Published online: 13 November 2017

Abstract

Objectives To determine the value of a 15-min delayed phase in extracellular contrast agent (ECA)-enhanced magnetic resonance imaging (MRI) for evaluation of hepatocellular carcinoma (HCC) in patients with chronic liver disease.

Methods Between 2014 and 2015, 103 patients with chronic liver disease underwent ECA-enhanced MRI; 133 lesions consisting of 107 HCCs, 23 benign lesions and three non-HCC malignancies were identified with pathological or clinical diagnosis. MRI images were reviewed by two abdominal radiologists independently using the European Association for the Study of the Liver (EASL) and Liver Imaging Reporting and Data System (LI-RADS) criteria. Imaging features observed in the 15-min delayed phase were recorded.

Results Of 107 HCCs, three or four additional HCCs were diagnosed according to the EASL criteria by adding the 15-min delayed phase, increasing sensitivity (Reviewer 1, from 69.2–72.0 % [P = 0.072]; Reviewer 2, from 75.7–79.4 % [P = 0.041]). Reviewers 1 and 2 upgraded one and four HCCs from LR-4 to LR-5 based on the LI-RADS, respectively. Among 23 benign lesions, no additional findings were observed in the 15-min delayed phase.

Conclusions Including the 15-min delayed phase in ECA-enhanced MRI may improve the diagnostic performance for HCC in patients with chronic liver disease.

Key Points

- *Additional acquisition of 15-min delayed phase (FDP) requires approximately 20 s.*
- *About 5 % of HCCs show washout or capsule appearance only in FDP.*
- *Including FDP improves the sensitivity of extracellular contrast agent-enhanced MRI for HCC.*
- *These results are applicable only to patients with chronic liver disease.*

Keywords Hepatocellular carcinoma · Gadoterate meglumine · Gadolinium DTPA · Magnetic resonance imaging · 15-minute delayed phase

Abbreviations

AASLD	American Association for the Study of Liver Diseases
ACR	American College of Radiology
AFP	Alpha-fetoprotein
CT	Computed tomography
EASL	European Association for the Study of the Liver
ECA	Extracellular contrast agent
FDP	Far (15-min) delayed phase
FN	False negative
FP	False positive
Gd-DOTA	Gadoterate meglumine
Gd-EOB-DTPA	Gadoxetic acid disodium
HBA	Hepatobiliary contrast agent
HBP	Hepatobiliary phase
HBV	Hepatitis B virus
HCC	Hepatocellular carcinoma
HCV	Hepatitis C virus

✉ Chansik An
chansikan@yuhs.ac; chansikan@gmail.com

[1] Department of Radiology, Research Institute of Radiological Science, Severance Hospital, Yonsei University, College of Medicine, 50-1 Yonsei-ro, Seodaemun-gu, Seoul 03722, Korea

LI-RADS	Liver Imaging Reporting and Data System
MRI	Magnetic resonance imaging
NA	Non-applicable
OM	Other hepatic malignancy
OPTN/UNOS	Organ Procurement and Transplantation Network/United Network for Organ Sharing
PACS	Picture archiving and communication system
TE	Echo time
TN	True negative
TP	True positive
TR	Repetition time

Introduction

Unlike other cancers, hepatocellular carcinomas (HCCs) can be diagnosed radiologically without histological confirmation. Several international scientific organisations or societies, including the European Association for the Study of the Liver (EASL), the American Association for the Study of Liver Diseases (AASLD), the American College of Radiology (ACR) and the Organ Procurement and Transplantation Network/United Network for Organ Sharing (OPTN/UNOS), have proposed different criteria for the imaging diagnosis of HCC, in which tumour size, arterial phase hyperenhancement, washout appearance and capsule appearance are major imaging features [1–4].

In the imaging diagnosis of hepatic malignancy, the accuracy of magnetic resonance imaging (MRI) for HCC is known to be superior to that of computed tomography (CT), and liver MRI is widely used for pre-treatment evaluation of patients with HCC [5–10]. Currently, two types of contrast agents are used for liver MRI: extracellular contrast agent (ECA) and hepatocyte-specific or hepatobiliary contrast agent (HBA). While ECAs such as gadoterate meglumine (Gd-DOTA) are distributed only in the intravascular and extracellular spaces before undergoing renal excretion, HBAs such as gadoxetic acid disodium (Gd-EOB-DTPA) are initially distributed in the extracellular space and then taken up by hepatocytes. The maximum hepatocyte uptake of gadoxetic acid, called the hepatobiliary phase (HBP), occurs 15–20 min after injection. The high contrast in signal intensity between hypointense focal lesions and the hyperintense surrounding liver in the HBP increases the diagnostic sensitivity of HBA-enhanced MRI [11–14].

In our institution, liver MRI is performed using ECA or HBA at the physician's discretion. The same protocol is used regardless of the type of contrast agent, and thus 15-min delayed-phase images are obtained for both ECA- and HBA-enhanced MRI. Additional acquisition of the 15-min delayed phase does not increase the scan time beyond approximately 20 s required for scanning one dynamic sequence, because we acquire T2-weighted and diffusion-weighted images between the late dynamic and the 15-min delayed phases.

In practice, we have observed that some hepatic lesions showing washout or capsule appearance only in the 15-min delayed phase of ECA-enhanced MRI were later confirmed as HCC. From these observations, we hypothesised that, if the imaging features observed only in the 15-min delayed phase are exclusively seen in HCC, including the 15-min delayed phase in the ECA-enhanced MRI protocol could help diagnose additional HCCs without making a false-positive diagnosis.

The purpose of this study was to examine the added value of the 15-min delayed phase of ECA-enhanced MRI for diagnosis of HCC in patients with chronic liver disease.

Materials and methods

Subjects

The institutional review board approved this retrospective study and waived the requirement for informed consent. Our database contained 2,188 patients with chronic liver disease who underwent liver MRI from January 2014 to December 2015. We excluded 2,008 patients who were previously treated for hepatic (n = 1,317) or other (n = 67) malignancies, who had no focal lesion other than definite benign lesions such as cysts or arterioportal shunts (n = 148), who underwent MRI using HBA (n = 339) or who were diagnosed with locally advanced or disseminated cancers (n = 141). A radiologist (H.S.H., with 3 years of experience in liver MRI) reviewed the MRI data of the remaining 176 patients and selected 304 suspicious focal hepatic lesions based on the prospectively written radiology reports. If a patient had more than five suspicious lesions, the five largest lesions with arterial phase hyperenhancement were selected. Among these 304 lesions, 171 observations were excluded from the analysis because their final diagnoses remained indeterminate (treated without pathological diagnosis [n = 77] or inconclusive follow-up [n = 94]; see 'Reference standards' section below). Our final study included 133 focal hepatic lesions from 103 patients (Fig. 1).

Reference standards

Patients' medical records and images were reviewed by a single investigator (H.S.H.) who determined the final diagnoses of the hepatic lesions. Histopathological diagnosis confirmed by surgery or biopsy was used as a reference standard. In cases for which histological diagnosis was not available, a hepatic lesion was diagnosed as HCC if it showed local or marginal

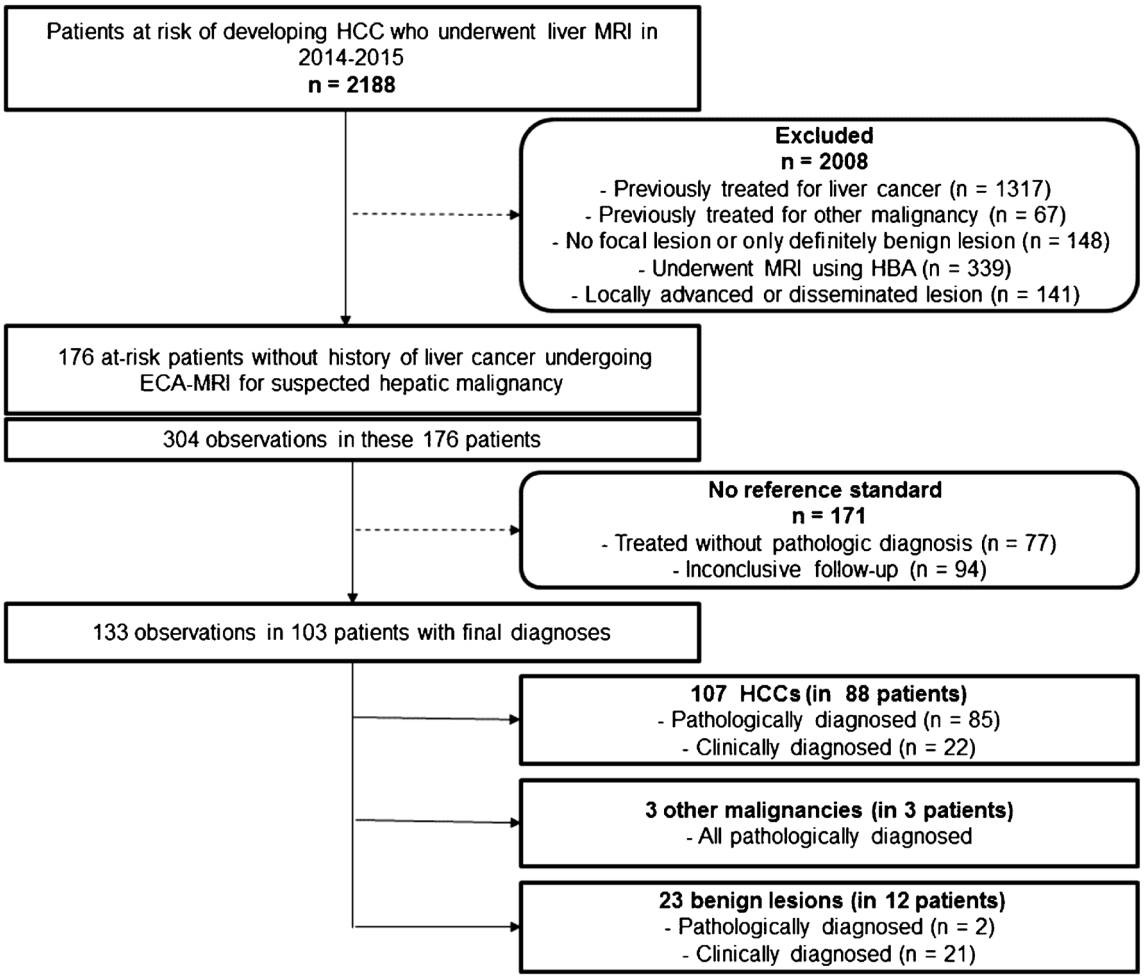

Fig. 1 Flowchart illustrating subject selection. *HBA* hepatobiliary contrast agent, *ECA* extracellular contrast agent, *HCC* hepatocellular carcinoma

recurrence after transarterial chemoembolisation or radiofrequency ablation, if it presented threshold growth (≥ 50 % diameter increase within 6 months or ≥ 100 % diameter increase over 6 months) [15, 16], or if it revealed new arterial phase hyperenhancement or washout appearance at follow-up. If a hepatic lesion disappeared or showed no interval change during a follow-up period of ≥ 18 months, it was considered benign [17].

MRI

MRI was conducted using three 3.0-T systems (MAGNETOM Trio, A Tim System, Siemens Medical Solutions, Erlangen, Germany; Intera Achieva, Koninklijke Philips N.V., Best, The Netherlands; Ingenia, Koninklijke Philips N.V.). All images were obtained in the transverse plane with a field of view of 44 × 33 cm or 40 × 30 cm depending on the patient's body size. After localiser images were taken, two-dimensional, dual-echo T1-weighted gradient-recalled echo images were acquired, with a slice thickness, intersection gap and repetition time (TR) of 7 mm, 0.7 mm and 150–192 ms, respectively. The echo times (TEs) for in-phase and opposed-phase images were 2.3–2.5 ms and 1.1–1.2 ms, respectively.

Pre- and post-contrast dynamic images were acquired using a three-dimensional gradient echo sequence with a section thickness, TR and TE of 2–4 mm, 2.5–4.5 ms and 0.9–2.2 ms, respectively. For dynamic imaging, an extracellular gadolinium-based contrast agent (Dotarem®, gadoterate meglumine, Guerbet, Aulnay-sous-Bois, France; Magnevist®, gadopentetate dimeglumin, Bayer Schering Pharma AG, Berlin, Germany) was injected at a dose of 0.2 ml/kg of body weight, followed by 20 ml of 0.9 % saline at an injection rate of 2 ml/s. The arterial phase began 3–5 s after peak contrast-enhancement of the abdominal aorta. The time-to-peak aorta enhancement was determined using a test bolus technique with 1 ml contrast

agent, or by obtaining bolus-tracking images. Images of three subsequent dynamic phases were acquired after arterial phase imaging: early portal phase, late portal phase and late dynamic phase with a breath-hold; the scan time of each phase was 18–24 s. The start times for scanning the arterial, early portal, late portal and late dynamic phases were 25–30 s, 65–75 s, 95–105 s and 135–150 s after contrast injection, respectively. In addition, the far delayed-phase images were acquired at a fixed time delay of 15 min after contrast injection using the same imaging sequence as dynamic T1-weighted imaging.

During the interval between the late dynamic and 15-min delayed-phase, T2-weighted images were acquired by multi-shot and single-shot turbo spin echo sequences using a navigator-triggered technique, with a section thickness, gap, TR and TE of 5–7 mm, 1 mm, 1,589–3,250 ms and 70–96 ms, respectively. Diffusion-weighted images were acquired using a navigator-triggered technique at b-values of 50, 400 and 800 s/mm^2.

Image analysis

All MRI images were retrospectively reviewed on a picture archiving and communication system (PACS; Centricity, Version 2.0, GE Healthcare, Barrington, IL, USA). A radiologist (H.S.H.) reviewed the pathology reports, surgical records and MRI data, and then recorded the location (hepatic segment), size and corresponding image number of each hepatic lesion. With this information, two board-certified abdominal radiologists (C.A. and M.J.K., with 6 and 23 years of experience in liver MRI, respectively) unaware of patients' clinical history or final diagnosis independently analysed the MRI images. For each hepatic lesion, they determined the presence or absence of arterial phase hyperenhancement, washout appearance and capsule appearance as defined by the Liver Imaging Reporting and Data System (LI-RADS) [3]. They also recorded imaging features observed in the 15-min delayed phase, including washout and capsule appearances. In addition, without referring to the 15-min delayed-phase images, they categorised each hepatic lesion according to the LI-RADS diagnostic algorithm proposed by the ACR [3]: LR-1 (definitely benign), LR-2 (probably benign), LR-3 (indeterminate), LR-4 (probable HCC), LR-5 (definite HCC), LR-5V (definite tumour in vein) or LR-M (probably malignant, but not specific for HCC).

Based on the results of the image analysis, an investigator who did not participate in image analysis (S.E.L.) categorised each hepatic lesion as HCC or non-HCC according to the EASL criteria, in which HCC is diagnosed if a hepatic lesion > 1 cm displays both arterial phase hyperenhancement and washout appearance [2], with and without using the imaging features found in the 15-min delayed phase. She also examined whether the hepatic lesions that had been categorised as LR-3 or LR-4 by the reviewers could be upgraded to LR-5 by considering the imaging features observed in the 15-min delayed phase. For imaging diagnosis using the LI-RADS, lesions categorised as LR-5 or LR-5V were considered positive for HCC.

Statistical analysis

The sensitivity, specificity and accuracy of the diagnostic criteria were calculated and compared using generalised estimating equations. Interobserver agreement was presented by Cohen's kappa coefficient. A kappa statistic of 0.8–1.0 was considered excellent agreement, 0.6–0.79 was good agreement, 0.40–0.59 was moderate agreement, 0.2–0.39 was fair agreement and 0–0.19 was poor agreement. Two-sided P-values < 0.05 were considered statistically significant. All statistical analyses were performed using SAS 9.2 (SAS Institute, Inc., Cary, NC, USA).

Results

Baseline characteristics

Our study population of 103 patients consisted of 77 men and 26 women; the median age was 61 years (range, 42–81 years). Hepatitis B virus was the most common cause of chronic liver disease (81.6 %), and most patients (88.3 %) were in Child-Pugh class A (Table 1). Of 133 hepatic observations in 103 patients, 107 (80.5 %) were HCCs, three (2.3 %) were other malignancies and 23 (17.3 %) were benign. Of the 107 HCCs, 85 (79.4 %) were pathologically diagnosed after hepatic resection (n = 66), liver transplantation (n = 18) or percutaneous biopsy (n = 1). The remaining 22 HCCs (20.6 %) were diagnosed according to the clinical criteria; 18 presented marginal recurrence at immediate follow-up after transarterial chemoembolisation or radiofrequency ablation, and four showed threshold growth with the radiological hallmark of HCC (i.e. arterial phase hyperenhancement and washout appearance) at follow-up. The three other malignancies were pathologically diagnosed as intrahepatic cholangiocarcinoma, combined HCC-cholangiocarcinoma and combined HCC-neuroendocrine carcinoma after hepatic resection. Of the 23 benign lesions, two (8.7 %) were pathologically confirmed to be regenerative and high-grade dysplastic nodules.

Inter-reader agreement of diagnosis was good regardless of the diagnostic criteria; kappa coefficients were 0.750 and 0.748 for the EASL and LI-RADS criteria, respectively.

Table 1 Characteristics of 103 patients with 133 hepatic lesions

Characteristics	Total
Patient	
Total number of patients	103
Age[a]	61 (42–81) years
Sex[b]	
Male	77 (74.8 %)
Female	26 (25.2 %)
Cause of chronic liver disease[b]	
HBV	84 (81.6 %)
HCV	10 (9.7 %)
HBV/HCV co-infection	3 (2.9 %)
Non-viral	6 (5.8 %)
Child-Pugh class[b]	
A	91 (88.3 %)
B	7 (6.8 %)
C	5 (4.9 %)
AFP level[a]	15.9 (1.3–224,633.9) ng/ml
Lesion	
Total number of lesions	133
Lesion size[a]	22.2 (4.9−192) mm
Final diagnosis[b]	
Hepatocellular carcinoma	107 (80.5 %)
Other malignancies	3 (2.3 %)
Benign	23 (17.3 %)

a Data are presented as number (%) for Sex, Cause of chronic liver disease, Child-Pugh class, Final diagnosis

b Data are presented as median (range) for Age, AFP level, Lesion size.

HBV hepatitis B virus, *HCV* hepatitis C virus, *AF*P alpha-fetoprotein

Imaging features observed only in the 15-min delayed phase

Reviewer 1 found washout appearance in three lesions and capsule appearance in three other lesions only in the 15-min delayed phase (Figs. 2 and 3). Reviewer 2 found washout appearance in one lesion, capsule appearance in two lesions, and both capsule and washout appearances in three lesions only in the 15-min delayed phase. All lesions that showed additional washout or capsule appearance in the 15-min delayed phase were confirmed as HCC. For one intrahepatic cholangiocarcinoma, both reviewers concluded that delayed phase central enhancement and peripheral washout appearance, imaging features favouring other hepatic malignancy over HCC, were unequivocally present only in the 15-min delayed phase (Fig. 4). None of the benign lesions or other malignancies showed additional washout or capsule appearance in the 15-min delayed phase. The frequencies of washout and capsule appearances observed in hepatic lesions with and without 15-min delayed-phase images are presented in Table 2.

Impact of the 15-min delayed phase on diagnostic performance

Using the EASL criteria, washout appearance observed only in the 15-min delayed phase resulted in three and four additional true-positive HCC diagnoses for Reviewers 1 and 2, respectively (Table 3). Consequently, the diagnostic sensitivity and accuracy improved by 2.8 % (P = 0.072) and 2.2 % (P = 0.080) for Reviewer 1, and by 3.7 % (P = 0.041) and 3.6 % (P = 0.042) for Reviewer 2, respectively. Using the LI-RADS criteria, one of six HCCs whose capsule appearances were only seen in the 15-min delayed phase was upgraded from LR-4 to LR-5 for Reviewer 1, minimally increasing the diagnostic sensitivity (P = 0.316) and accuracy (P = 0.315); three HCCs were upgraded from LR-3 to LR-4. For Reviewer 2, washout or capsule appearance seen only in the 15-min delayed phase upgraded four HCCs from LR-4 to LR-5, increasing the sensitivity and accuracy by 3.7 % (P = 0.043) and 3.1 % (P = 0.042), respectively; one HCC was upgraded from LR-3 to LR-4 (Table 3).

There was no additional false-positive case due to imaging features observed in the 15-min delayed phase, irrespective of the diagnostic criteria or the reviewer. Thus, the diagnosis of benign or other malignant lesions was not affected, and the diagnostic specificity did not change due to the additional use of the 15-min delayed phase (Table 3).

Discussion

In the present study, approximately 5 % of HCCs manifested washout or capsule appearance only in the 15-min delayed phase; some resulted in additional true-positive diagnoses or upgrades in the LI-RADS category, without additional false-positive diagnoses. We believe this diagnostic benefit is sufficient to compensate for the additional scan time of 18–24 s needed for acquisition of 15-min delayed-phase images in ECA-enhanced MRI.

Although the underlying mechanism of washout appearance in HCC is not yet fully understood, it may be partly explained by the combination of various effects, including venous drainage of contrast media, background liver enhancement due to the retention of contrast media within fibrotic parenchyma, tumoral hypercellularity with corresponding reduction in extracellular volume, and intrinsic hypoattenuation or hypointensity [18, 19]. Capsule appearance, which is defined as a peripheral rim of smooth hyperenhancement in the portal venous or delayed phase of dynamic contrast-enhanced imaging, reflects the retention of contrast media within peritumoral fibrosis and prominent sinusoids surrounding a tumour [20]. Progressive concentric enhancement and delayed central enhancement, which are features favouring other

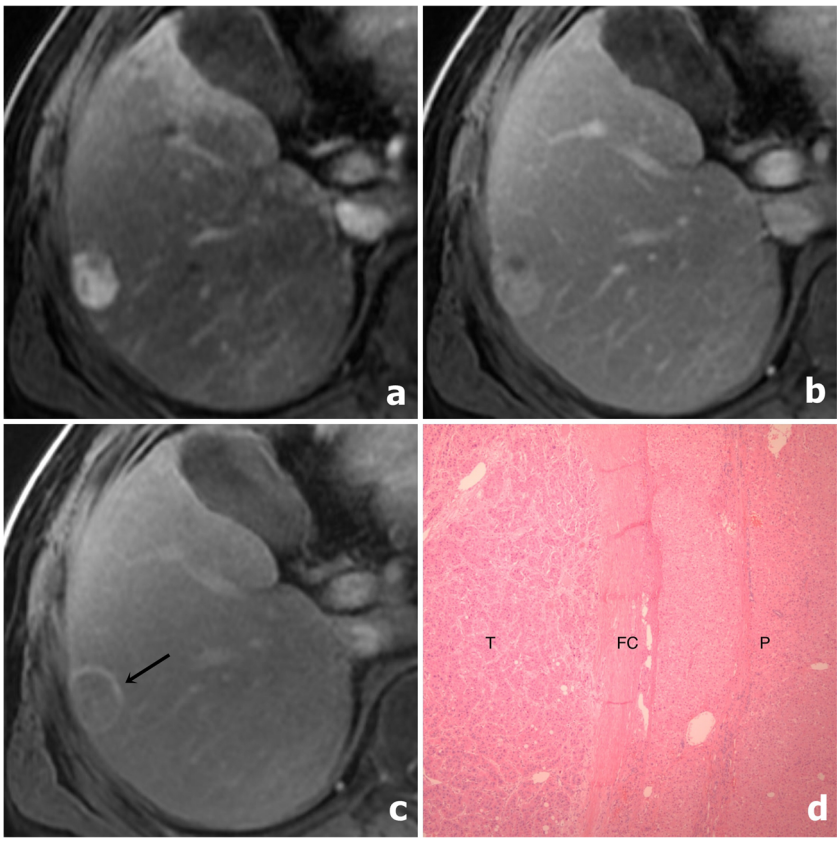

Fig. 2 A hepatocellular carcinoma in a 59-year-old man with B-viral liver cirrhosis; our reviewers concluded that capsule appearance is unequivocally observed only in the 15-min delayed phase of extracellular contrast agent-enhanced MRI. (**a**) A 2.4-cm mass in the right posterior liver shows arterial phase hyperenhancement. (**b**) No capsule is seen in the portal or late dynamic phases. (**c**) The mass displays smooth, ring-like enhancement (arrow) in the 15-minute delayed phase. (**d**) Microscopic examination after resection shows a fibrous capsule (FC) between the tumour (T) and the normal parenchyma (P) (haematoxylin-eosin stain; original magnification, ×20)

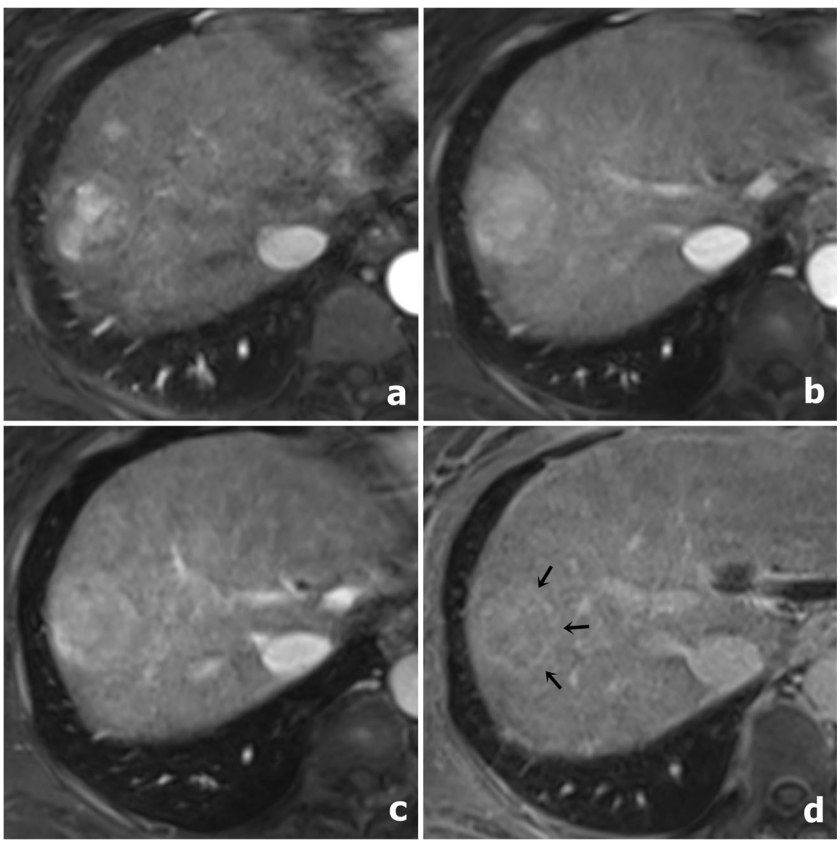

Fig. 3 A hepatocellular carcinoma in a 69-year-old women with B-viral liver cirrhosis; our reviewers concluded that capsule and washout appearances are present only in the 15-min delayed phase of extracellular contrast agent-enhanced MRI. (**a**) A 3.3-cm mass in the hepatic dome shows diffuse arterial phase hyperenhancement. (**b** and **c**) No capsule appearance is seen in the portal (**b**) or late dynamic (**c**) phases. (**d**) Capsule appearance (arrows) is present in the 15-min delayed phase, and one reviewer also concluded that washout appearance is present in this phase

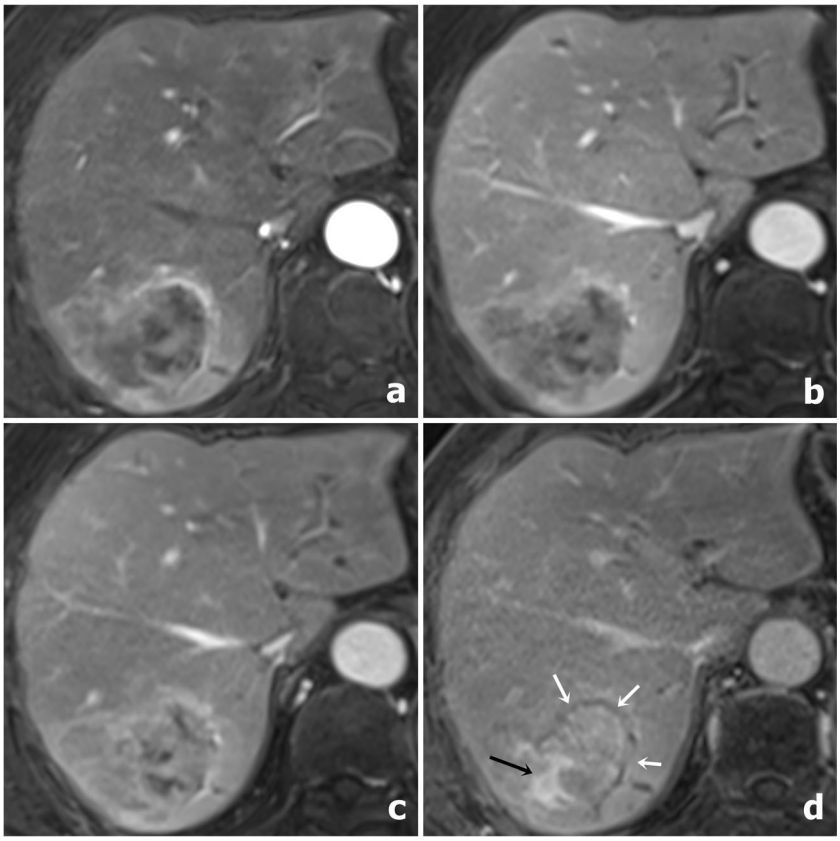

Fig. 4 An intrahepatic cholangiocarcinoma in a 67-year-old man with B-viral liver cirrhosis; imaging features are prominently visible in the 15-min delayed phase of extracellular contrast agent-enhanced MRI. (**a**) A 4.5-cm mass with irregular rim-like arterial phase hyperenhancement is seen in the right posterior liver. (**b** and **c**) No specific imaging findings other than subtle progressive contrast enhancement are noted in the portal (**b**) and late dynamic (**c**) phases. (**d**) In the 15-min delayed-phase, peripheral washout appearance (white arrows) and delayed-phase central enhancement (black arrow), features that favour other hepatic malignancy over hepatocellular carcinoma, are visible

malignancy such as cholangiocarcinoma over HCC, are due to the retention of contrast media in central stromal fibrosis [21].

From the mechanisms explained above, it can be inferred that a certain amount of time is required after contrast injection for these imaging features to be unequivocally exhibited. Although the time required may vary depending on the characteristics of each lesion and the surrounding liver parenchyma, the imaging features likely become more apparent as time passes after contrast injection. In the early years after the introduction of multi-detector CT for HCC diagnosis, several groups reported that some HCCs showed a washout appearance only in the 3- or 5-min delayed phase of ECA-enhanced CT, and that the diagnostic sensitivity and accuracy could be improved by adding delayed-phase imaging to the biphasic CT [22–26]. Afterwards, some investigators demonstrated that imaging features observed in the 10-min or longer delayed phase might be helpful in distinguishing HCC from other hepatic lesions [27, 28]. Other investigators reported that

Table 2 Frequencies of washout and capsule appearances on extracellular contrast agent-enhanced MRI with and without the 15-min delayed phase

		Reviewer 1		Reviewer 2	
Imaging feature	Diagnosis	Without 15-min delayed phase	With 15-min delayed phase	Without 15-min delayed phase	With 15-min delayed phase
Washout appearance	HCC	73.8 % (79/107)	76.6 % (82/107)	82.2 % (88/107)	86.0 % (92/107)
	OM	66.7 % (2/3)	66.7 % (2/3)	100 % (3/3)	100 % (3/3)
	benign	65.2 % (15/23)	65.2 % (15/23)	52.2 % (12/23)	52.2 % (12/23)
Capsule appearance	HCC	46.7 % (50/107)	49.5 % (53/107)	75.7 % (81/107)	80.4 % (86/107)
	OM	66.7 % (2/3)	66.7 % (2/3)	100 % (3/3)	100 % (3/3)
	benign	0 % (0/23)	0 % (0/23)	1.7 % (4/23)	1.7 % (4/23)

HCC hepatocellular carcinoma, *OM* other hepatic malignancy

Table 3 Diagnostic performance of extracellular contrast agent-enhanced MRI with and without the 15-min delayed phase according to EASL and LI-RADS criteria

	Reviewer 1				Reviewer 2			
	TP/TN/FP/FN	Sensitivity	Specificity	Accuracy	TP/TN/FP/FN	Sensitivity	Specificity	Accuracy
EASL for HCC diagnosis								
Without 15-min phase	74/24/2/33	69.2 %	92.3 %	73.7 %	81/23/3/26	75.7 %	88.5 %	78.2 %
With 15-min phase	77/24/2/30	72.0 %	92.3 %	75.9 %	85/23/3/22	79.4 %	88.5 %	81.8 %
P-value		0.072	NA	0.080		0.041	NA	0.042
LI-RADS for HCC diagnosis								
Without 15-min phase	66/25/1/41	61.7 %	96.2 %	68.4 %	78/25/1/29	72.9 %	96.2 %	77.4 %
With 15-min phase	67/25/1/40	62.6 %	96.2 %	69.2 %	82/25/1/25	76.6 %	96.2 %	80.5 %
P-value		0.316	NA	0.315		0.043	NA	0.042

EASL European association for the study of the liver, *LI-RADS* liver imaging reporting and data system, *TP* true positive, *TN* true negative, *FP* false positive, *FN* false negative, *HCC* hepatocellular carcinoma, *NA* non-applicable

imaging features of intrahepatic cholangiocarcinoma could be better detected 10 min after contrast injection [29, 30], like the case we have experienced in this study.

Previously, it was not practical to include a long delayed phase in imaging protocols, because it would mean waiting until the delayed phase, doing nothing. Currently, however, liver MRI routinely includes T2-weighted and diffusion-weighted imaging, which can be acquired between the late dynamic (i.e. 3-min delayed) phase and 15-min delayed phase (or hepatobiliary phase for HBA-enhanced MRI) without compromising the diagnostic performance [14, 31–33]. Therefore, in ECA-enhanced MRI, we believe that the benefits of acquiring 15-min delayed images outweigh its costs.

A major limitation of this study was its retrospective nature. We excluded 171 observations due to the lack of pathological diagnosis or inconclusive follow-up during subject selection. Furthermore, some HCC and benign lesions were diagnosed using the non-pathological criteria, because the current guidelines permit non-invasive imaging diagnosis of HCC in at-risk patients. In addition, the reviewers were aware they were investigating the possible effects of a 15-min delayed phase on diagnostic accuracy. All these potential biases arising from the retrospective nature of this study might have led to the overestimation of diagnostic accuracy of ECA-enhanced MRI applying the 15-min delayed phase.

In conclusion, the additional use of 15-min delayed-phase images may enable diagnosis of more HCCs using ECA-enhanced MRI, as some HCCs display typical imaging features later than in the conventional delay time of 3 min after contrast injection.

Compliance with ethical standards

Guarantor The scientific guarantor of this publication is Myeong-Jin Kim.

Conflict of interest The authors of this manuscript declare no relationships with any companies whose products or services may be related to the subject matter of the article.

Funding This study was supported by a grant from the National R&D Program for Cancer Control, Ministry of Health & Welfare, Republic of Korea (Grant #1520160).

Statistics and biometry One of the authors has significant statistical expertise.

Informed consent Written informed consent was waived by the Institutional Review Board.

Ethical approval Institutional Review Board approval was obtained.

Methodology
- retrospective
- diagnostic or prognostic study
- performed at one institution

References

1. Bruix J, Sherman M (2011) Management of hepatocellular carcinoma: an update. Hepatology 53:1020–1022
2. European Association For The Study Of The Liver (2012) EASL–EORTC clinical practice guidelines: management of hepatocellular carcinoma. J Hepatol 56:908–943
3. American College of Radiology. Liver Imaging Reporting and Data System. http://www.acr.org/Quality-Safety/Resouces/LIRADS. Accessed 10 Apr 2017
4. Wald C, Russo MW, Heimbach JK, Hussain HK, Pomfret EA, Bruix J (2013) New OPTN/UNOS policy for liver transplant allocation: standardization of liver imaging, diagnosis, classification, and reporting of hepatocellular carcinoma. Radiology 266:376–382
5. Colli A, Fraquelli M, Casazza G et al (2006) Accuracy of ultrasonography, spiral CT, magnetic resonance, and alpha-fetoprotein in diagnosing hepatocellular carcinoma: a systematic review. Am J Gastroenterol 101:513–523

6. Lee YJ, Lee JM, Lee JS et al (2015) Hepatocellular carcinoma: diagnostic performance of multidetector CT and MR imaging—a systematic review and meta-analysis. Radiology 275:97–109
7. Vilgrain V, Esvan M, Ronot M, Caumont-Prim A, Aube C, Chatellier G (2016) A meta-analysis of diffusion-weighted and gadoxetic acid-enhanced MR imaging for the detection of liver metastases. Eur Radiol 26:4595–4615
8. Zech CJ, Justo N, Lang A et al (2016) Cost evaluation of gadoxetic acid-enhanced magnetic resonance imaging in the diagnosis of colorectal-cancer metastasis in the liver: Results from the VALUE Trial. Eur Radiol 26:4121–4130
9. Kim R, Lee JM, Shin CI et al (2016) Differentiation of intrahepatic mass-forming cholangiocarcinoma from hepatocellular carcinoma on gadoxetic acid-enhanced liver MR imaging. Eur Radiol 26: 1808–1817
10. Park HJ, Jang KM, Kang TW et al (2016) Identification of Imaging Predictors Discriminating Different Primary Liver Tumours in Patients with Chronic Liver Disease on Gadoxetic Acid-enhanced MRI: a Classification Tree Analysis. Eur Radiol 26:3102–3111
11. Ahn SS, Kim MJ, Lim JS, Hong HS, Chung YE, Choi JY (2010) Added value of gadoxetic acid-enhanced hepatobiliary phase MR imaging in the diagnosis of hepatocellular carcinoma. Radiology 255:459–466
12. Haimerl M, Wachtler M, Platzek I et al (2013) Added value of Gd-EOB-DTPA-enhanced Hepatobiliary phase MR imaging in evaluation of focal solid hepatic lesions. BMC Med Imaging 13:41
13. Phongkitkarun S, Limsamutpetch K, Tannaphai P, Jatchavala J (2013) Added value of hepatobiliary phase gadoxetic acid-enhanced MRI for diagnosing hepatocellular carcinoma in high-risk patients. World J Gastroenterol 19:8357–8365
14. Neri E, Bali MA, Ba-Ssalamah A et al (2016) ESGAR consensus statement on liver MR imaging and clinical use of liver-specific contrast agents. Eur Radiol 26:921–931
15. An C, Rakhmonova G, Choi JY, Kim MJ (2016) Liver imaging reporting and data system (LI-RADS) version 2014: understanding and application of the diagnostic algorithm. Clin Mol Hepatol 22: 296–307
16. Choi SH, Byun JH, Lim YS et al (2016) Diagnostic criteria for hepatocellular carcinoma 3 cm with hepatocyte-specific contrast-enhanced magnetic resonance imaging. J Hepatol 64:1099–1107
17. An C, Choi YA, Choi D et al (2015) Growth rate of early-stage hepatocellular carcinoma in patients with chronic liver disease. Clin Mol Hepatol 21:279–286
18. Choi JY, Lee J-M, Sirlin CB (2014) CT and MR imaging diagnosis and staging of hepatocellular carcinoma: part I. Development, growth, and spread: key pathologic and imaging aspects. Radiology 272:635–654
19. Choi JY, Lee JM, Sirlin CB (2014) CT and MR imaging diagnosis and staging of hepatocellular carcinoma: part II. Extracellular agents, hepatobiliary agents, and ancillary imaging features. Radiology 273:30–50
20. Ishigami K, Yoshimitsu K, Nishihara Y et al (2009) Hepatocellular carcinoma with a pseudocapsule on gadolinium-enhanced MR images: correlation with histopathologic findings. Radiology 250: 435–443
21. Jeong HT, Kim MJ, Chung YE, Choi JY, Park YN, Kim KW (2013) Gadoxetate disodium–enhanced MRI of mass-forming intrahepatic cholangiocarcinomas: imaging-histologic correlation. AJR Am J Roentgenol 201:W603–W611
22. Mitsuzaki K, Yamashita Y, Ogata I, Nishiharu T, Urata J, Takahashi M (1996) Multiple-phase helical CT of the liver for detecting small hepatomas in patients with liver cirrhosis: contrast-injection protocol and optimal timing. AJR Am J Roentgenol 167:753–757
23. Hwang GJ, Kim MJ, Yoo HS, Lee JT (1997) Nodular hepatocellular carcinomas: detection with arterial-, portal-, and delayed-phase images at spiral CT. Radiology 202:383–388
24. Kim T, Murakami T, Takahashi S et al (1999) Optimal phases of dynamic CT for detecting hepatocellular carcinoma: evaluation of unenhanced and triple-phase images. Abdom Imaging 24:473–480
25. Lim JH, Choi D, Kim SH et al (2002) Detection of hepatocellular carcinoma: value of adding delayed phase imaging to dual-phase helical CT. AJR Am J Roentgenol 179:67–73
26. Monzawa S, Ichikawa T, Nakajima H, Kitanaka Y, Omata K, Araki T (2007) Dynamic CT for detecting small hepatocellular carcinoma: usefulness of delayed phase imaging. AJR Am J Roentgenol 188:147–153
27. Yoshida H, Itai Y, Ohtomo K, Kokubo T, Minami M, Yashiro N (1989) Small hepatocellular carcinoma and cavernous hemangioma: differentiation with dynamic FLASH MR imaging with Gd-DTPA. Radiology 171:339–342
28. Peterson MS, Murakami T, Baron RL (1998) MR imaging patterns of gadolinium retention within liver neoplasms. Abdom Imaging 23:592–599
29. Keogan MT, Seabourn JT, Paulson EK, McDermott VG, Delong DM, Nelson RC (1997) Contrast-enhanced CT of intrahepatic and hilar cholangiocarcinoma: delay time for optimal imaging. AJR Am J Roentgenol 169:1493–1499
30. Lacomis JM, Baron RL, Oliver JH 3rd, Nalesnik MA, Federle MP (1997) Cholangiocarcinoma: delayed CT contrast enhancement patterns. Radiology 203:98–104
31. Choi JS, Kim MJ, Choi JY, Park MS, Lim JS, Kim KW (2010) Diffusion-weighted MR imaging of liver on 3.0-Tesla system: effect of intravenous administration of gadoxetic acid disodium. Eur Radiol 20:1052–1060
32. Saito K, Araki Y, Park J et al (2010) Effect of Gd-EOB-DTPA on T2-weighted and diffusion-weighted images for the diagnosis of hepatocellular carcinoma. J Magn Reson Imaging 32:229–234
33. Cha DI, Jang KM, Kim SH, Kang TW, Song KD (2017) Liver Imaging Reporting and Data System on CT and gadoxetic acid-enhanced MRI with diffusion-weighted imaging. Eur Radiol. https://doi.org/10.1007/s00330-017-4804-1